Effects of detector size and position on a test of Born's rule using a three-slit experiment

Etienne Gagnon, Christopher D. Brown, and Amy L. Lytle[*]

Department of Physics and Astronomy, Franklin & Marshall College, P.O. Box 3003, Lancaster, Pennsylvania 17604, USA

(Received 17 March 2014; published 23 July 2014)

Recent high-precision measurements in a three-slit diffraction experiment [Sinha *et al.*, Science **329**, 418 (2010)] have been performed as an explicit test of the validity of Born's rule for quantum probabilities. This experiment aims to establish an upper limit to the possibility of higher-order interference, which, if observed, could support generalization of quantum probability theory. We reproduce this three-slit experiment using position-resolved detection, compare our results to a computational model, and find significant limitations to the normalization scheme proposed by Sinha *et al.* that influence interpretation. We further show that the dependence of the measurements on detector size and position must be taken into account for proper interpretation of results and meaningful comparison with other experimental schemes.

I. INTRODUCTION

Early in the development of quantum mechanics, Born proposed [1] a physical interpretation of Schrödinger's quantum wave function as "a density of probability for the presence of a particle" [2]. Using the well-understood mathematics of classical wave theory, he showed that, given this interpretation, Schrödinger's wave mechanics was mathematically equivalent to the more controversial matrix mechanics he was developing with Heisenberg. The classic example demonstrating the similarity in the behavior of classical wave and quantum particles is the double-slit experiment [3]. According to Born, the probability of detecting a photon is analogous to optical intensity, so that the absolute square of the quantum wave-function amplitude is analogous to the absolute square of the electric field amplitude. When any quantum particles travel through a pair of slits, the probability of detecting each particle at a screen on the far side forms an interference pattern like that formed by any classical wave encountering the same setup. The presence of interference indicates a wavelike quantum superposition, in contrast with a particlelike, classical sum of probabilities.

Born's rule has been incredibly successful in predicting such outcomes in quantum mechanics, although, since its proposal in 1926, it has neither been definitively derived from first principles [4], nor explicitly experimentally tested, until recently. In 1994, Sorkin [5] noted the following remarkable result that follows from Born's rule (see Ref. [6] for a straightforward derivation). While the probability distribution observed in a two-slit experiment is not a simple sum of those observed when only one of the slits is open, the probability distribution for *three* slits *can* be written as a sum (with appropriate minus signs) of those for each of the cases when only one or two of the three slits is open. In other words, there is no interference unique to the presence of three (or more) open slits (or, in general, any three or more mutually exclusive quantum paths). Demonstration of the existence of such higher-order interference would violate Born's rule and have extensive ramifications for quantum theory. This idea has inspired a number of proposed and realized experimental tests

[6–11] of Born's rule, as well as a number of discussions of the implications of a generalized probability theory [12–14].

Sinha *et al.* [6] have reported the first such experimental test of Born's rule using the three-slit scheme outlined by Sorkin. The magnitude of a possible higher-order interference is given by

$$\epsilon(\mathbf{r}) = p_{ABC}(\mathbf{r}) - p_{AB}(\mathbf{r}) - p_{BC}(\mathbf{r}) - p_{CA}(\mathbf{r}) + p_A(\mathbf{r})$$
$$+ p_B(\mathbf{r}) + p_C(\mathbf{r}) - p_0(\mathbf{r}), \qquad (1)$$

where $p_X(\mathbf{r})$ is the optical intensity as a function of position $\mathbf{r}$ in the plane of detection. The subscript indicates which of the three slits (A, B, and/or C) is open, while $p_0(\mathbf{r})$ accounts for background light scatter and dark counts in the detector. Born's rule predicts that, in the far-field approximation [15], $\epsilon(\mathbf{r}) = 0$ at all positions $\mathbf{r}$. Any nonzero value for ϵ found from combining these eight measurements that is not attributable to experimental error would indicate the existence of higher-order interference. This null test has the advantage of being independent of the exact experimental parameters such as shape and size of the slits or wavelength of the light, eliminating the need to know these parameters to a high degree of precision. On the other hand, a null test requires a thorough characterization and understanding of the possible sources of experimental uncertainty, and how they will affect interpretation of the results.

Sinha *et al.* further propose a normalized variant of ϵ, $\kappa(\mathbf{r}) = \epsilon(\mathbf{r})/\delta(\mathbf{r})$, where

$$\delta(\mathbf{r}) = |p_{AB}(\mathbf{r}) - p_A(\mathbf{r}) - p_B(\mathbf{r})| + |p_{BC}(\mathbf{r}) - p_B(\mathbf{r})$$
$$- p_C(\mathbf{r})| + |p_{CA}(\mathbf{r}) - p_C(\mathbf{r}) - p_A(\mathbf{r})| \qquad (2)$$

is the sum of the three possible combinations of two-slit interference terms, which are assumed to be nonzero. This normalization quantifies the *possible* three-path interference as a percentage of the *expected* two-path interference. Such a measure is intended to facilitate comparison between different experimental realizations of detecting higher-order interference, including different geometries for photons [8,10] as well as particles [9,11].

In this paper, we report an experimental and computational reproduction of this three-slit experiment in the semiclassical regime, in which we investigate the interpretation of these parameters given position-resolved measurement of the

_____

[*]alytle@fandm.edu

interference patterns. We show that in order to interpret experimental results using δ for normalization, one must take into account the fact that, while generally nonzero for either classical or quantum waves, the value of δ in the three-slit experiment varies with position in the plane of detection. Furthermore, the magnitude of δ varies with the size of the detector, or, in other words, the width of the interference pattern that is integrated. In fact, in the limit of a very small detector, δ tends toward zero at any detector position, in a way that causes the proposed normalization to obscure how reduced error affects the value of ϵ. A simulation modeling likely sources of random and systematic error in our experiment shows excellent agreement with our experimental results, and underscores the need to consider position-dependent sources of error in the three-slit experiment. Finally, we discuss why, independent of the normalization scheme used, position-resolved detection is required for a definitive characterization of possible violations to Born's rule.

II. EXPERIMENT

The experimental setup, shown schematically in Fig. 1, is based on the work of Sinha *et al.*, with some variations. Most significantly, we use a one-dimensional CCD array as a detector. The CCD (Thorlabs LC1-USB) has 3000 elements, with a 7-μm pitch and 7-μm pixel size. A sample three-slit diffraction pattern is shown in Fig. 1. For comparison with similar three-slit experiments, we define our position variable in terms of the characteristic size of features in the diffraction pattern, the principal fringe period (PFP). In our setup, the PFP is $\sim$617 μm, so the 7-μm pitch of our CCD corresponds to $\sim$1.1% of the PFP. The raw data are then used to calculate the values of ϵ, δ, and κ as a function of position and detector size.

The light source was a $\sim$5-mW HeNe laser (632.8 nm). In order to produce each of the eight interference patterns required for calculating ϵ, δ, and κ, a blocking mask actuated by a microstepper motor was placed in front of the stationary diffraction slits. Both sets of apertures were machined from a 25-μm-thick stainless steel sheet, and were separated by a propagation distance of approximately 2 mm. The dimensions of the apertures were chosen so that at this separation distance, each slit was illuminated by a narrow section of the near-field diffraction produced by a single opening in the mask. A cylindrical lens focused the diffracted light onto the detector located $\sim$39 cm from the slits, well into the far field. Each set of eight diffraction patterns was measured 200 times to minimize statistical error. In each scan of eight measurements, the order was changed randomly in order to mitigate systematic errors from slow drifts in the system, such as those in optical intensity or alignment.

An experiment testing a quantum-mechanical principle such as Born's rule requires the use of very low flux in order to test the particle nature of light. Our measurements are performed instead in the semiclassical regime due to the low sensitivity of our detector. Nevertheless, our findings are relevant in both regimes, as we are examining effects that will be present in the experiment whether or not Born's rule holds perfectly. We do not presume to claim a limit on the validity of Born's rule in this work, but instead are concerned with how the data are interpreted.
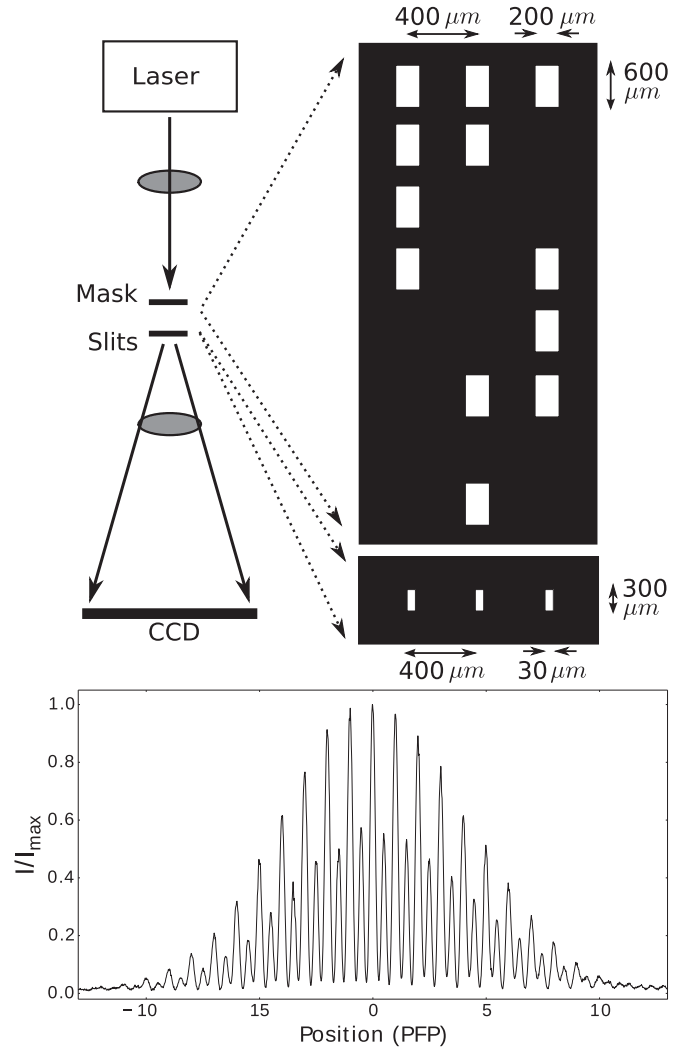

FIG. 1. Experimental setup. The different combinations of open and closed slits are achieved by adjusting the position of the mask with respect to the stationary three slits. Dimensions of the slits and mask apertures are shown at right. (Bottom) Typical diffraction pattern corresponding to all three slits open [$p_{ABC}(\mathbf{r})$].

III. DATA AND ANALYSIS

A. Influence of detector size

The size of the detector relative to the features of the interference patterns has a direct influence on the value determined as an upper limit to violations of Born's rule. The detection probability, or, classically, the phase shift between different contributions to the total amplitude, varies continuously with position in the detection plane. Using as small a detector as possible makes sense experimentally, both to reduce experimental error and to probe as narrow a range of phase differences as possible. Practically, however, the detector will have some finite size and will therefore integrate optical intensity over a range of phase differences between waves propagating from the different slits. In general, a smaller detector size will yield a smaller upper limit to violations to Born's rule, hence the need for normalization. The proposed normalization parameter δ, however, varies with detector size
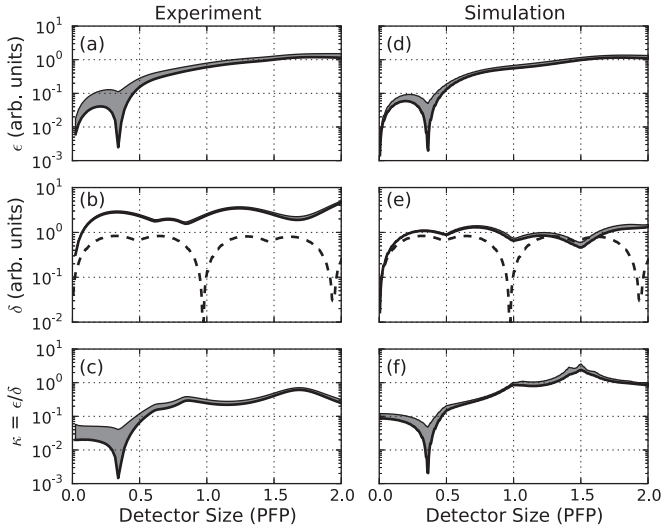
FIG. 2. Measured (a–c) and simulated (d–f) ϵ, δ, and κ as a function of detector size. The gray-shaded region indicates one standard deviation above the mean. Dashed lines indicate δ calculated in the absence of any error.

by definition and in fact approaches zero for some detector sizes, including those arbitrarily small. This leads to the fact that δ obscures and distorts the behavior of ϵ, making κ an ill-defined parameter for comparison with other experimental schemes.

The CCD array allowed us to investigate the effects of both detector size and experimental error on the measured values of ϵ, δ, and κ. We "vary" the size of the detector by binning the raw data from a varying number of pixels before calculating each parameter. The data shown in Figs. 2(a)–2(c) represent a detector centered on the central peak of the diffraction pattern, with a width of $(2n + 1) \times 7\ \mu$m, where n is an integer, and $7\ \mu$m is the width of a single pixel.

The main structures of the data shown in Figs. 2(a)–2(c) can be attributed to the presence of both random and systematic errors that are proportional to the optical intensity. The dominant sources suspected in our experiment originate with the relative alignment between the blocking mask and the slits. Mechanical vibration due the movement of the microstepper motor will change their relative positions, leading to random sampling by the slits of the near-field diffraction of the mask apertures. Systematic variation in the transmission of different slit combinations is evident when comparing the relative intensities of the individual diffraction patterns. The motion of the translation stage may introduce a systematic variation due to the lateral alignment between the slits and mask, or scattering from the mask mount. With these types of error, the monotonic increase in the magnitudes of both ϵ and δ with increased detector size can be attributed to accumulation of error over increasingly larger regions of the CCD. As expected, smaller detector sizes limit the accumulation of error and its effect on the value of ϵ and hence κ, but the variations in δ with detector size clearly alter the behavior of κ in comparison to ϵ.

To better understand how different sources of error affect the values of these parameters, we modeled our experiment

with a computer simulation that included various suspected sources of random and systematic error. The model was based on a Fourier-transform beam propagation method, in which we assume a classical, monochromatic plane wave incident on the blocking mask and ignore the vector nature of the field. For direct comparison with our experimental data, we used the physical parameters of the slits, blocking mask, and beam path described in the experimental section above. The position resolution of the simulated irradiance at the detector was ∼0.005 PFP. Random error due to mechanical vibrations were included as random variation in the lateral position of the slits (by as much as ±10 μm) and in the distance between the mask and slits (by as much as ±10 μm). Systematic error due to misalignment was included as a systematic variation in the distance between the mask and slits, which varied by a distance of 50 μm between each position of the mask. We also included a systematic variation in the effective transmission of each of the seven mask aperture sets, based on the best fit to the relative intensities of the individual interference patterns. The data shown here included 100 samples.

The simulated results, shown in Figs. 2(d)–2(f), reproduce many of the same features, which, in the case of ϵ, are due purely to experimental error. The variance due to the random error qualitatively behaves the same; a precise match would require better knowledge of the noise spectrum. Some of the structure of the variation of δ with detector size, however, is present even in the absence of experimental error. The dashed curve in Figs. 2(b) and 2(e) show the simulated δ with no errors included. Here, the monotonic increase due to the accumulation of error is absent. However, δ exhibits a significant variation with detector size, which translates to κ, even when experimental errors are minimized. The choice of δ as a normalization factor is problematic, not only because δ is not constant, but also because it approaches zero for detector sizes that are integer multiples of the principal fringe period, including when the size of the detector approaches zero.

The interference term for two-slit diffraction in the far-field approximation is sinusoidal:

$$I_{AB}(x) = p_{AB}(x) - p_A(x) - p_B(x) = C_{AB}\cos\left(\frac{2\pi x}{L_{AB}}\right),$$

(3)

where x is the position in the plane of detection, L_{AB} is the spatial period of the interference pattern, and C_{AB} is a constant dependent on the laser power and the size of the slits. When δ is measured, this signal is integrated over a finite region of the detection plane. An integration region that is equal to any integer multiple of the principal fringe period will yield $\delta = 0$ for any position x, since this is an integer multiple of the spatial period for each pair of slits: $L_{AB} = L_{BC} = 2L_{AC}$. When the single-slit diffraction envelope is included in this analysis, the value of δ will not be exactly zero but will nonetheless decrease to a small value, the magnitude depending on the ratio of the slit width to slit spacing. For the slit geometry of our experiment, δ decreases by 2 orders of magnitude relative to its maximum value at a detector size of 1 PFP.

When the detector size is close to the fringe spacing, then the value of κ will be large at any position in the detection plane. This effect is in fact more problematic as experimental
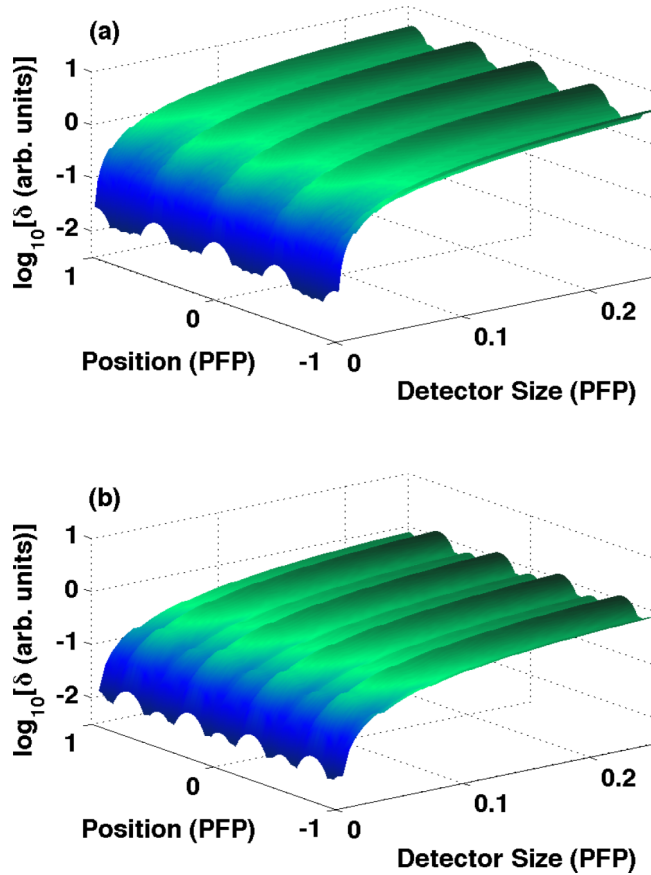
FIG. 3. (Color online) Calculated δ as a function of both position and detector size, given (a) our experimental parameters and (b) Sinha *et al.*'s experimental parameters, with no simulated experimental error.

error is reduced, since δ will approach its theoretically small value. Even when enough error is present to prevent such small values for δ, its behavior is nonetheless mapped onto κ, as can be seen in Figs. 2(c) and 2(f).

This implies that, at the very least, detector sizes close to an integer multiple of the principal fringe period should be avoided. As discussed earlier, the smaller the detector size, the smaller the error, so that normalization is required for meaningful comparison between experiments. But δ as defined also approaches zero as the detector size approaches zero. Figure 3 shows how δ varies both with detector size and position, with no modeled experimental error, for detector sizes ranging from approximately 0.005 to 0.25 PFP.

Both our experimental and simulated data show that this variation in δ as the detector size approaches zero introduces a serious limitation to its usefulness as a normalization. We find that, for detector sizes smaller than about 0.1 PFP, ϵ decreases approximately linearly with detector size due to a reduction in accumulated error, while δ decreases approximately linearly with detector size by definition. This means that κ levels off to a constant, nonzero value, obscuring the fact that ϵ, the more direct measure of the error, continues to decrease [see Figs. 2(c) and 2(f)]. This effect is consistent for any position in the detection plane, and for any type or magnitude of error we modeled we used our simulation to model.

As a specific example showing this effect even for highly precise experimental conditions, we model Sinha *et al.*'s experimental parameters, the results of which are shown in Figs. 4(a)–4(c). We included the dominant systematic error described in their report (a defect in the blocking mask, in which one of the apertures was offset by 8 μm), and random error due to mechanical vibration (a variation of up to ± 0.5 μm in the lateral position of the slits, as well as the distance between the mask and slits). In the absence of detailed information about the uncertainties in the experiment of Ref. [6], we have chosen a conservative level of error that is consistent with the precision of results reported. While it may not model their results precisely, our model is representative of how these types of errors affect interpretation of the results.

As expected, ϵ decreases to zero as the detector size decreases. With such a small magnitude of error, δ varies from its error-free shape (shown as a dashed line) by at most a few percent. κ, however, tends toward a constant, nonzero value. Thus, even though the experimental error is very small and has been further reduced through the use of a smaller detector, the normalization prevents κ from reflecting this.

The remaining plots of Fig. 4 illustrate how this effect is consistent across all positions of the interference pattern. Figures 4(d)–4(f) show the simulation's results using the detector size of Sinha *et al.*, which was 0.04 PFP, and for comparison, Figs. 4(g)–4(i) show the results for a detector size of 0.005 PFP, around the size of a typical CCD pixel or single-mode fiber. In reducing the size of the detector, the values of ϵ and δ both drop by roughly an order of magnitude, but κ remains the same. What this implies is that if Sinha *et al.* were to replace their multimode fiber in the detection with a single-mode fiber, they would predict exactly the same upper limit for κ (our simulation predicts 0.01 ± 0.04 in both cases), when in fact they had reduced their uncertainty by an order of magnitude (ϵ decreases from 0.03 ± 0.10 to 0.003 ± 0.011).

B. Influence of detector position

In alternative experimental schemes for testing Born's rule using three-path interference [9–11], the phase differences between the three different quantum paths are well defined for a given measurement and thus avoid the problems introduced by the detector size. In any experimental scheme, however, κ will have variations that are dependent on the relative phase shifts between quantum paths. In the three-slit scheme, this corresponds to the position of the detector within the interference patterns. Position-dependent variations come from two main sources: first, the fact that δ varies with position as it is defined, and second, that the experimental uncertainties of both ϵ and δ also vary with position.

First, two-slit interference, and therefore δ, varies with position by definition, as can be seen in Fig. 3. For all detector widths, the variation in magnitude differs by, at most, a factor of approximately 2 when comparing different detector positions. If the upper limit on the existence of three-slit interference is quoted as an order of magnitude, this variation may not be significant, but as the experimental errors are reduced, the variation in δ with detector position will become more evident. Authors of previous work [7,8] have noted that δ can take on a small value at specific detector positions, causing
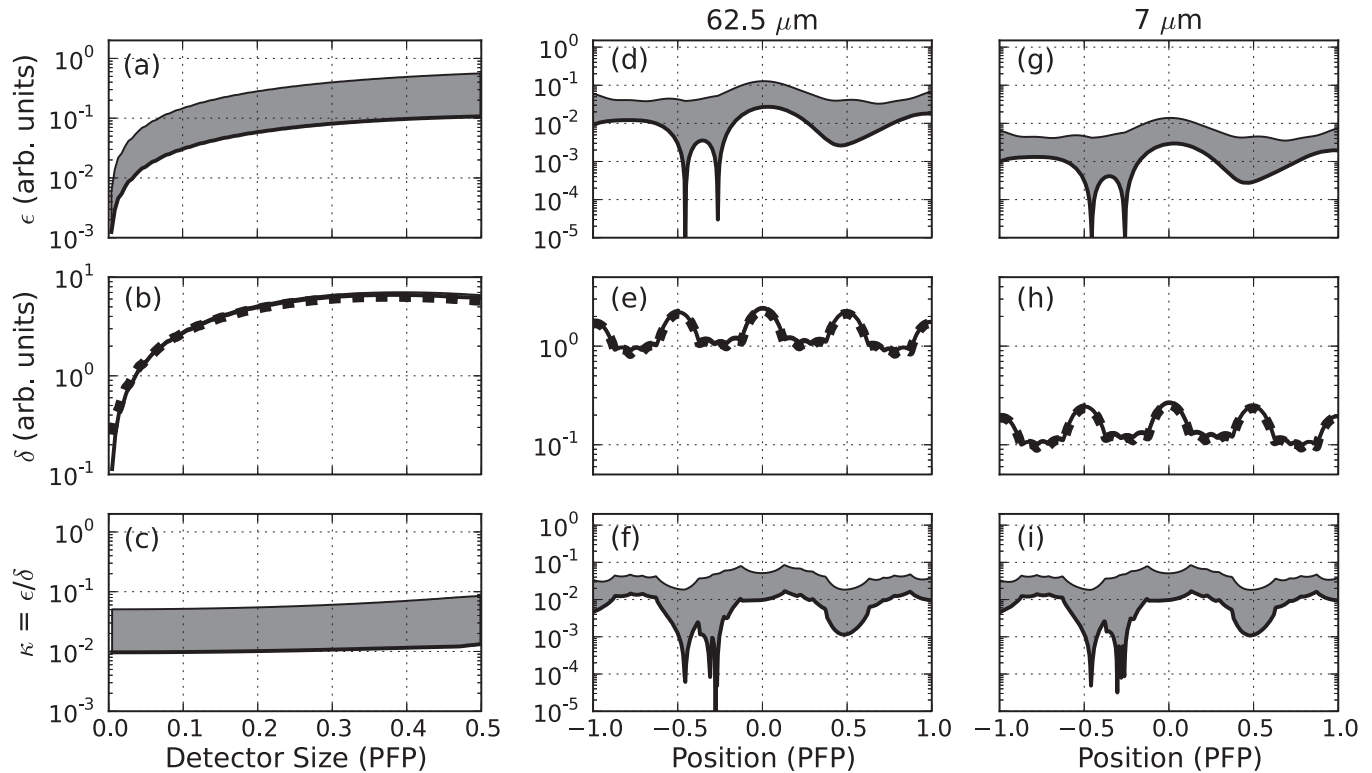
FIG. 4. Simulated ϵ, δ, and κ as a function of detector size (a–c) and position (d–f), given the experimental parameters and systematic error in the mask described in [6]. Plots (g–i) show how reducing the size of the detector from 62.5 to 7 μm changes these parameters. The gray-shaded region indicates one standard deviation above the mean. Dashed lines indicate δ calculated in the absence of any error.

a large value for κ that might be dismissed as anomalous, but δ's systematic dependence on detector position can also affect interpretation of results. Our simulations confirm that as experimental error is reduced, κ becomes more and more reflective of δ, as opposed to the uncertainty in ϵ. Without understanding how the position dependence of δ affects κ, this structure could be misinterpreted as a third-order interference pattern.

Another problematic aspect of δ as defined is that its dependence on position varies with the particular experimental geometry chosen. Figure 3 shows how the position dependence of δ differs for the two geometries of the three-slit experiment discussed in this paper, but its dependence may be different still for experimental schemes other than three-slit interference. Hence, it is impossible to provide a straightforward characterization of how δ will influence the results, even for variations in the geometry of the three-slit experiment.

Second, experimental uncertainty will be position-dependent for those errors proportional to the optical intensity. In Fig. 5 we show our experimental data alongside our simulation results, including suspected sources of error, as a function of position. The fact that the nonzero values for ϵ have the same spatial periodicity as the interference patterns suggests that they can be attributed to errors proportional to intensity. This systematic error also affects the shape of δ, as can be seen when comparing the experimental data (solid line) in Fig. 5(b) to the simulation results with no error (dashed line). Importantly, however, the position dependence of the systematic error will be *different* for ϵ and δ, as they are each measuring different position-dependent signals. These differences in position dependence will then be

juxtaposed in the uncertainty of κ, making interpretation more difficult.

While defining the normalization as the ratio of three-slit to two-slit interference is intuitively appealing for the purposes of comparison between experiments using different quantum systems, it is problematic, and in fact becomes more so as the experimental design is improved and uncertainty reduced. A
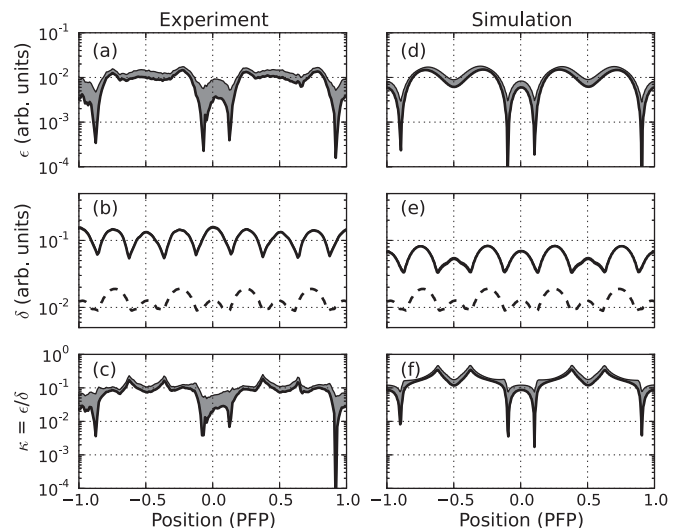

FIG. 5. Measured (a–c) and simulated (d–f) ϵ, δ, and κ as a function of position. The gray-shaded region indicates one standard deviation above the mean.

simpler choice for normalization may be the magnitude of the intensity at the central peak of the three-slit interference pattern. This would correspond, in other experimental schemes, to zero phase shift among the three quantum paths. This value would be constant, nonzero, and avoid the problems associated with position and detector-size dependence.

C. The need for position-resolved detection

Regardless of the normalization scheme, calculations and measurements over a wider phase space are needed for a definitive characterization of an upper bound to violations of Born's rule. There are two major problems with probing a single detector position. First, the magnitude of the experimental error in the three-slit experiment depends on the position. This is evident for the types of error based on alignment uncertainty we have simulated, simulations of detector nonlinearity, as shown previously [7], or in our experimental data [see Fig. 2(a)]. If the upper bound on the presence of higher-order interference is determined by the experimental uncertainty, then this will be valid only for the detector position chosen.

As a representative example of how different the results can be depending on where in the pattern the measurements are made, even when the error is small, we consider again the predictions of the simulation using the experimental parameters of Sinha *et al.* Figure 4(d) indicates that the error varies by several orders of magnitude over 2 PFP, but it seems reasonable that measurements would be easiest to perform at an interference maximum, so we compare two such locations. At the center of the interference pattern, the value of ϵ predicted by our simulation was 0.03 ± 0.10, while at the first secondary maximum ($+0.5$ PFP) it was 0.003 ± 0.038. The corresponding values for κ were 0.010 ± 0.042 and $0.001\,0 \pm 0.018$. While it could be argued that measurements at the center of the interference pattern give the largest, and thus the most conservative estimate of the error, this is not always the case, as the position dependence of the errors is sensitive to the type and magnitude of errors present, as well as the experimental geometry used. Compare, for example, Fig. 4(d) to the results of our experiment shown in Figs. 5(a) and 5(d), in which the largest values for ϵ and κ are not at the center of the interference pattern.

Second, a hypothetical higher-order interference may also be position dependent, just as two-slit interference is position dependent. In the absence of any theoretical prediction about where it is likely to detect a nonzero interference, the choice of a single detector position may yield a zero value for ϵ, simply because it coincides with a "minimum" of the three-slit interference term. Either of these problems would inaccurately

support claims on the upper bound to violations of Born's rule. Precise measurements and propagation of error over a range of phase differences is needed.

Finally, recent work has called into question the premises of Refs. [5,6] that lead to the conclusion that ϵ is exactly zero, and thus that a detected nonzero result would necessarily show violation of Born's rule. Precise numerical modeling of Maxwell's equations predicts a nonzero ϵ in the classical regime [15], and numerical modeling of Feynman's path integral formalism predicts a nonzero result in the quantum regime [16], while both are consistent with Born's rule. In either case, the nonzero result is several orders of magnitude smaller than the measurement precision demonstrated to date. However, in more precise experiments, these effects must be taken into account. In both cases, the results are also position dependent, and definitive testing of either theory would be most strongly supported by position-resolved data.

IV. CONCLUSION

We have investigated the three-slit experiment for testing Born's rule using position-resolved detection of the interference patterns. Experimental data show that uncertainties due to experimental error in the parameters ϵ, δ, and κ show significant dependence on the position and detector size. A numerical simulation to model these experimental errors shows good agreement with our measured data. These results reveal limitations to the use of the previously proposed normalization factor based on two-slit interference δ and indicate that these limitations are robust and persist even as experimental uncertainty is reduced. Additionally, we conclude that a single number, while convenient for comparison between experimental schemes, is an insufficient measure for quantifying possible violations to Born's rule. Indeed, position-resolved measurement of ϵ is necessary to validate Born's rule, since a three-term interference signal may itself be position dependent. If unrecognized, these position-dependent effects could lead to false interpretation in the pursuit of a more precise upper bound to violations of Born's rule. A complete test of Born's rule using this experimental approach will require measurement at the single-photon level, with a more straightforward normalization scheme, and statistics calculated over a full range of phase differences.

[1] M. Born, Zeitschrift fur Physik **37**, 863 (1926).

[2] J. A. Wheeler and W. H. Zurek, *Quantum Theory and Measurement* (Princeton University Press, Princeton, NJ, 1983).

[3] R. P. Feynman, R. B. Leighton, and M. Sands, *The Feynman Lectures on Physics* (Addison-Wesley, Reading, MA, 1964).

[4] *Compendium of Quantum Physics*, edited by D. Greenberger, K. Hentschel, and F. Weinert (Springer-Verlag, Berlin, 2009).

[5] R. Sorkin, Mod. Phys. Lett. A **9**, 3119 (1994).

[6] U. Sinha, C. Couteau, T. Jennewein, R. Laflamme, and G. Weihs, Science **329**, 418 (2010).

[7] U. Sinha, C. Couteau, Z. Medendorp, I. Söllner, R. Laflamme, R. Sorkin, and G. Weihs, in *Foundations of Probability and Physics-5*, CP1101 (AIP, Melville, New York, 2009).

[8] J. M. Hickmann, E. J. S. Fonseca, and A. J. Jesus-Silva, Europhys. Lett. **96**, 64006 (2011).

[9] D. K. Park, O. Moussa, and R. Laflamme, New J. Phys. **14**, 113025 (2012).

[10] I. Söllner, B. Gschösser, P. Mai, B. Pressl, Z. Vörös, and G. Weihs, Found. Phys. **42**, 742 (2012).

[11] J. Klepp, Y. Tomita, C. Pruner, J. Kohlbrecher, and M. Fally, Appl. Phys. Lett. **101**, 154104 (2012).

[12] C. Ududec, H. Barnum, and J. Emerson, Found. Phys. **41**, 396 (2011).

[13] G. Jaeger, Found. Phys. **42**, 752 (2012).

[14] G. Niestegge, Found. Phys. **43**, 805 (2013).

[15] H. De Raedt, K. Michielsen, and K. Hess, Phys. Rev. A **85**, 012101 (2012).

[16] R. Sawant, J. Samuel, A. Sinha, S. Sinha, and U. Sinha, arXiv:1308.2022v1 [quant-ph].